Robust Adaptive High-Order Geometric and Numerical Methods Based on Weighted Least Squares

Xiangmin (Jim) Jiao

Department of Applied Mathematics & Statistics and
Institute for Advanced Computational Science
Stony Brook University

March 24, 2016

Computational Challenges in Aerosciences

Two of six areas in NASA CFD technology roadmap:[1]

- Numerical Algorithms
  - "Discretization techniques such as **higher-order accurate methods** offer the potential for better accuracy and scalability, although **robustness** and **cost considerations** remain"
  - "Linear and nonlinear solvers ... that are ... **near optimal**", including extension of "**Krylov methods**, **highly parallel multigrid methods**"
- Geometry and Grid Generation
  - ... "remains one of the **most important bottlenecks** for large-scale complex simulations"
  - "**Curved** mesh elements for **higher order methods**", "**tight CAD coupling** and production **adaptive mesh refinement** (AMR)", "**disruptive ideas** such as anisotropic cut-cell meshes"

These two areas are intimately related, at both theoretical and practical levels, and require a holistic approach.

[1] J. Slotnick, A. Khodadoust et al., CFD Vision 2030 Study: A Path to Revolutionary Computational Aerosciences, NASA/CR–2014-218178.

Sources of Challenges: Complex Geometry and Multiphysics

- Scientific applications often involve complex geometries

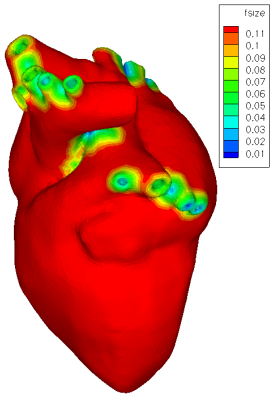


- Complex geometries pose significant challenges
  - Robustness and accuracy of numerical methods
  - Productivity and efficiency of modeling and simulations
- Many systems are multiphysics
  - Different physics may require different numerical techniques
  - Lack of unification of numerical methods causes difficulties in coupling

Challenges in Numerical Methods

- Classical finite difference methods
  - Developed for regular grids discretizing simple domains
  - Require special treatments near (curved) boundaries
- Finite element methods (and most variants)
  - Work for irregular domains; widely used
  - Require high element quality
- Finite volume methods
  - Specifically for hyperbolic conservation laws
  - More challenging to achieve high-order accuracy
- These challenges are inter-related, and many are rooted in the **centuries-old interpolation-based approximation theory**
- Other methods have emerged recently: meshless methods, radial basis functions, moving least squares, etc., but inefficient or inaccurate

Overview of Our Approach

1. Unified theoretical framework based on weighted-least squares (WLS)
2. Advanced geometric and numerical methods
3. Efficient algorithms and implementations

Representative Publications

- R. Conley, T.J. Delaney, and X. Jiao, Overcoming Element Quality Dependence of Finite Elements with AES-FEM, *Int. J. Num. Meth. in Engrg.*, in press, 2016.
- H. Liu and X. Jiao, WLS-ENO for Finite Volume Methods on Unstructured Meshes. *J. Comput. Phys.*, in press, 2016.
- X. Jiao and D. Wang, Reconstructing High-Order Surfaces for Meshing, *Engineering with Computers*, 2012.
- C. Lu, X. Jiao, and N. Missirlis, A hybrid geometric+algebraic multigrid method, *Num. Lin. Alg. Appl.*, 2014.

Outline

A Historical Perspective of Numerical Approximations

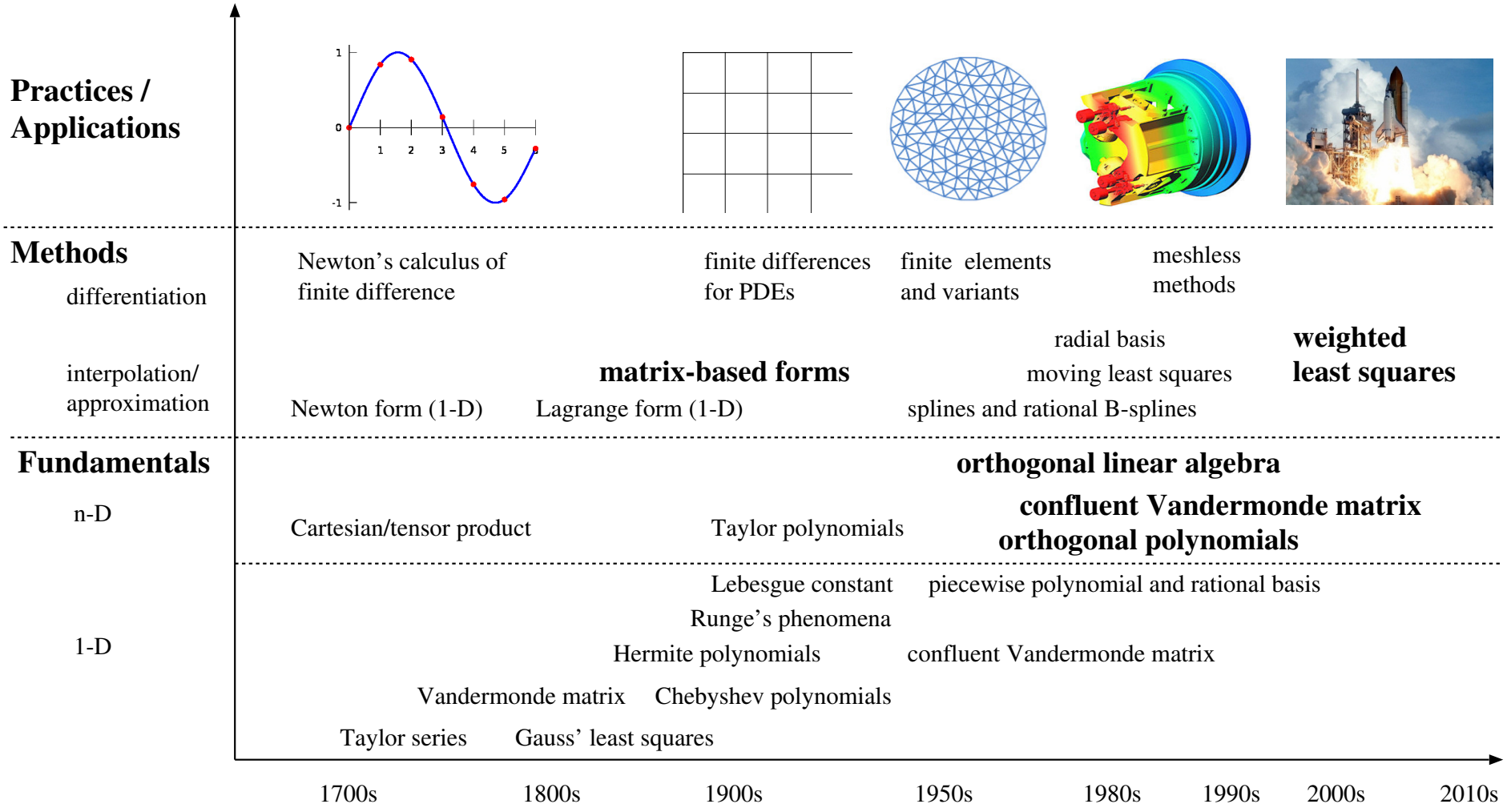

- We propose to use WLS-based approximations, which are accurate and stable, and are applicable to irregular stencils

A Fundamental Question of Numerical Approximations

- Given *stencil* $\boldsymbol{X} = \{\boldsymbol{x}_k\}$ around $\boldsymbol{x}_0 \in \mathbb{R}^d$ and a set of basis functions $\Phi(\boldsymbol{x}) = \{\phi_j(\boldsymbol{x})\}$, find

$$\tilde{f}(\boldsymbol{x}) = \sum_{i=1}^{n} c_i \phi_i(\boldsymbol{x}),$$

  to approximate $f(\boldsymbol{x}) : \mathbb{R}^d \to \mathbb{R}$ about $\boldsymbol{x}_0$, by determining $\boldsymbol{c}$ from finite number of known values of f at points $\boldsymbol{x}_k \in \boldsymbol{X}$
- After obtaining $\boldsymbol{c}$, approximate any *linear differential operator* $\mathcal{L}$ at $\boldsymbol{x} = \boldsymbol{x}_0 + \delta\boldsymbol{x}$ by

$$\mathcal{L}\, f(\boldsymbol{x}_0 + \delta\boldsymbol{x}) \approx \mathcal{L}\, \tilde{f}(\boldsymbol{x}_0 + \delta\boldsymbol{x}) = \sum_{i=1}^{n} c_i \left(\mathcal{L}\, \phi_i(\delta\boldsymbol{x})\right)$$

- Finite difference, finite element, finite volume methods all utilize this construction locally by computing $\boldsymbol{c} = \{c_i\}$ from interpolation

Overview of Weighted Least Squares (WLS)

- Consider *weighting scheme* $w(\boldsymbol{x}) : \mathbb{R}^d \to \mathbb{R}^+$, so that $w_k = w(\boldsymbol{x}_k)$ assigns a *weight* to $\boldsymbol{x}_k \in \boldsymbol{X}$. $(\boldsymbol{X}, \boldsymbol{w})$ is a *weighted stencil*
- To obtain $\boldsymbol{c}$, WLS minimizes weighted Sobolev norm

$$\min \sum_{\boldsymbol{x}_k \in \boldsymbol{X}} \left(w_k \sum_{\boldsymbol{\alpha}_j} s_j |\tilde{f}^{(\boldsymbol{\alpha}_j)}(\boldsymbol{x}_k) - f^{(\boldsymbol{\alpha}_j)}(\boldsymbol{x}_k)|^2 \right),$$

  where $f^{(\boldsymbol{\alpha}_j)}$ denotes partial derivative for $\boldsymbol{\alpha}_j \in \mathbb{N}^d$, $\tilde{f}^{(\boldsymbol{\alpha}_j)} = \sum_i c_i \phi_i^{(\boldsymbol{\alpha}_j)}$, and s_j is scaling factor for $f^{(\boldsymbol{\alpha}_j)}$
- This leads to linear least squares problem for $\boldsymbol{c}$, which we solve using orthogonal linear algebra techniques
- If matrix is nonsingular, it reduces to interpolation or Hermite interpolation
- *WLS* provides a unified framework over irregular, weighted stencils on unstructured meshes or point clouds

Algebraic Equations of WLS Formulation

- Convert WLS to linear system $\boldsymbol{A}\boldsymbol{c} \approx \boldsymbol{W}\boldsymbol{b}$
  - $\boldsymbol{A} = \boldsymbol{W}\hat{\boldsymbol{V}}$ is the product of following matrices
    - ★ $\boldsymbol{W}$: weighting matrix composed of w_k
    - ★ $\hat{\boldsymbol{V}}$: *confluent Vandermonde matrix* of $\delta\bar{\boldsymbol{x}} \in [-1, 1]^d$ in basis Φ
  - $\boldsymbol{b}$ contains scaled $s_j f^{(\boldsymbol{\alpha}_j)}(\boldsymbol{x}_k)$
  - Its solution is $\boldsymbol{c} = \boldsymbol{A}^+\boldsymbol{W}\boldsymbol{b}$
- Let $\boldsymbol{a}(\boldsymbol{x}) = \mathcal{L}\,\Phi(\delta\bar{\boldsymbol{x}})$ and $\boldsymbol{d}(\boldsymbol{x}) = \boldsymbol{W}\boldsymbol{A}^{+T}\boldsymbol{a}(\boldsymbol{x})$. Then

$$\begin{aligned} \mathcal{L}\,\tilde{f}(\boldsymbol{x}_0 + \delta\boldsymbol{x}) &= \boldsymbol{c}^T\boldsymbol{a}(\boldsymbol{x}) && (1) \\ &= \boldsymbol{b}^T\boldsymbol{d}(\boldsymbol{x}) && (2) \end{aligned}$$

  - (1) is *explicit differentiation*
  - (2) is *implicit differentiation* (or *finite difference formula*)
  - $\boldsymbol{d}(\boldsymbol{x})$ is *generalized Lagrange basis function*

Outline

Unified Weighted-Residual Formulation for PDEs

- Consider abstract but general form of linear, time-independent PDE

$$\mathcal{P}\, u(\boldsymbol{x}) = f(\boldsymbol{x}),$$

  with boundary conditions, where $\mathcal{P}$ is linear differential operator
- In a *weighted residual method*, given a set of test functions $\Psi(\boldsymbol{x}) = \{\psi_j(\boldsymbol{x})\}$, we obtain one equation for each ψ_j as

$$\int_\Omega \mathcal{P}\, u(\boldsymbol{x})\, \psi_j d\boldsymbol{x} = \int_\Omega f(\boldsymbol{x})\, \psi_j d\boldsymbol{x}.$$

- Boundary conditions are applied by modifying the linear system
- In *Galerkin finite elements*, ψ_j are finite-element shape functions
- In *(generalized) finite differences*, ψ_j are Dirac delta functions at nodes
- In *finite volumes*, ψ_j are step functions over control volume

Algebraic Equations from Weighted-Residual Methods

- Introduce basis functions $\Phi(\boldsymbol{x}) = \{\phi_i(\boldsymbol{x})\}$ to approximate u and f
- Suppose $\Phi = [\phi_1, \phi_2, \ldots, \phi_n]^T$ and $\Psi = [\psi_1, \psi_2, \ldots, \psi_n]^T$
- Let $u \approx \boldsymbol{u}^T \Phi = \sum_i u_i \phi_i$, and similarly $f(\boldsymbol{x}) \approx \sum_i f_i \phi_i$
- PDE leads to linear system $\boldsymbol{A}\boldsymbol{u} = \boldsymbol{b}$, where

$$A_{ij} = \int_\Omega \psi_i(\boldsymbol{x})\, \mathcal{P}\, \phi_j(\boldsymbol{x}) d\boldsymbol{x} \quad \text{and} \quad b_i = \int_\Omega f(\boldsymbol{x}) \psi_i(\boldsymbol{x}) d\boldsymbol{x}$$

- In FEM, $\int_\Omega \psi_i(\boldsymbol{x})\, \mathcal{P}\, \phi_j(\boldsymbol{x}) d\boldsymbol{x}$ is often transformed to $\int_\Omega \mathcal{L}_1 \psi_i(\boldsymbol{x}) \cdot (\mathcal{L}_2\, \phi_i(\boldsymbol{x}))^T\, d\boldsymbol{x}$ via integration by parts

We use WLS-based basis functions, and in turn generalize finite difference, finite element, and finite volume methods.

Overcoming Element-Quality Dependency of FEM

- FEM is workhorse in engineering, but its accuracy, stability, and efficiency heavily depends on element shapes, so engineers often spend $> 60\%$ of time on meshing

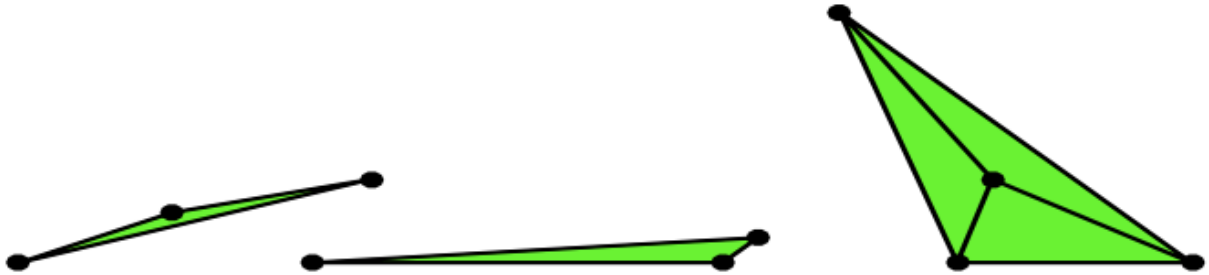

Examples of poor-shaped elements in 2-D and 3-D.

- This dependency is due to interpolation-based basis functions
- We propose *Adaptive Extended-Stencil FEM* to overcome this issue

Overview of Adaptive Extended-Stencil FEM

- Basic Idea of Adaptive Extended-Stencil FEM (AES-FEM)[2]
  - Preserve overall framework, including weak form, test functions, quadrature rules, ways to enforce boundary conditioners, etc.
  - Replace Lagrange basis functions in FEM with *generalized Lagrangian polynomial* (*GLP*) basis functions constructed using WLS over adaptive, extended neighborhood at each node

Definition

Given a set of degree-d polynomial basis functions $\{\phi_i\}$, we say it is a set of degree-d *generalized Lagrange polynomial (GLP) basis functions* if:

1. $\sum_i f(x_i)\phi_i$ approximates a function f to $\mathcal{O}\left(h^{d+1}\right)$ in a neighborhood of the stencil, where h is some characteristic length measure, and
2. $\sum_i \phi_i = 1$.

[2] R. Conley, T.J. Delaney, and X. Jiao, Overcoming Element Quality Dependence of Finite Elements with Adaptive Extended Stencil FEM (AES-FEM), *Int. J. Num. Meth. in Engrg.*, in press, 2016. DOI: 10.1002/nme.5246.

Examples of Adaptive, Extended Stencils

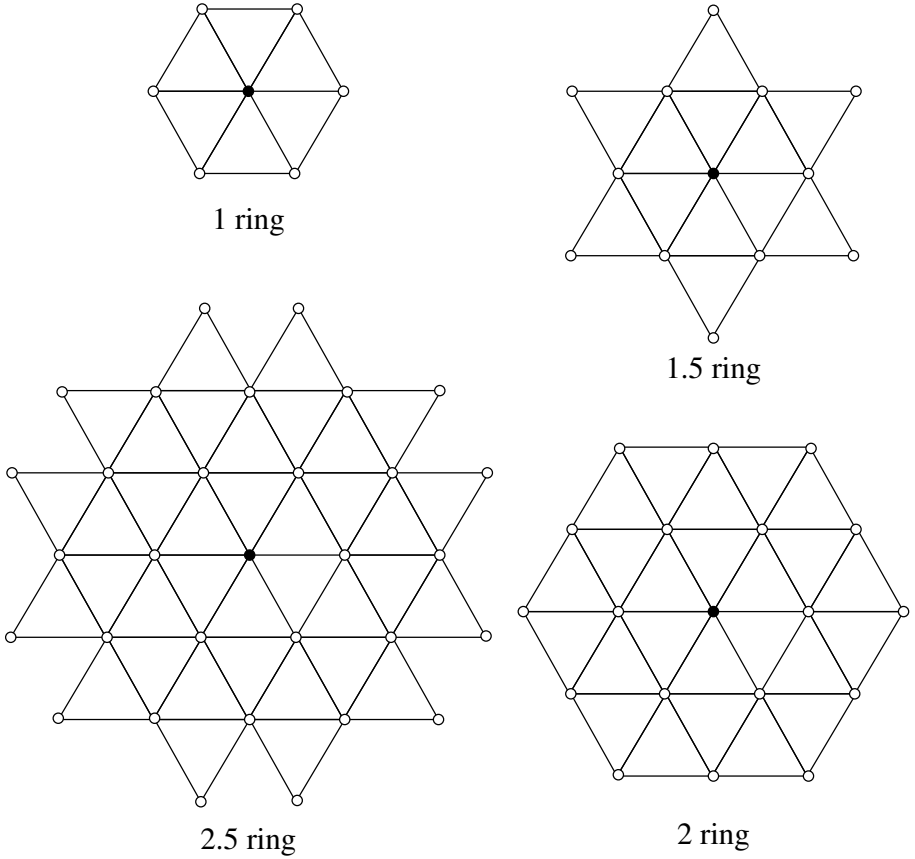

- In 2-D, use 1, 1.5, 2 & 2.5 rings for degree-2, 3, 4 & 5, respectively
- In 3-D, define rings at 1/3 increments for better granularity
- Adaptively enlarge stencils if WLS is ill-conditioned

Properties of AES-FEM

Theorem

Suppose u is smooth and thus $\|\nabla u\|$ is bounded. Then, when solving the Poisson equation using AES-FEM with degree-d GLP basis functions, for each ψ_i the weak form is approximated to $\mathcal{O}(h^d)$, where h is some characteristic length measure of the mesh.

- With similar sparsity pattern, AES-FEM allows higher-order basis functions than those of FEM, and hence enables better accuracy
- For its extended stencil, AES-FEM is insensitive to element shapes.

Comparison of Accuracy of AES-FEM vs. FEM

Poisson equation

$$-\nabla^2 u = f \quad \text{in } \Omega$$
$$u = g \quad \text{on } \partial\Omega$$

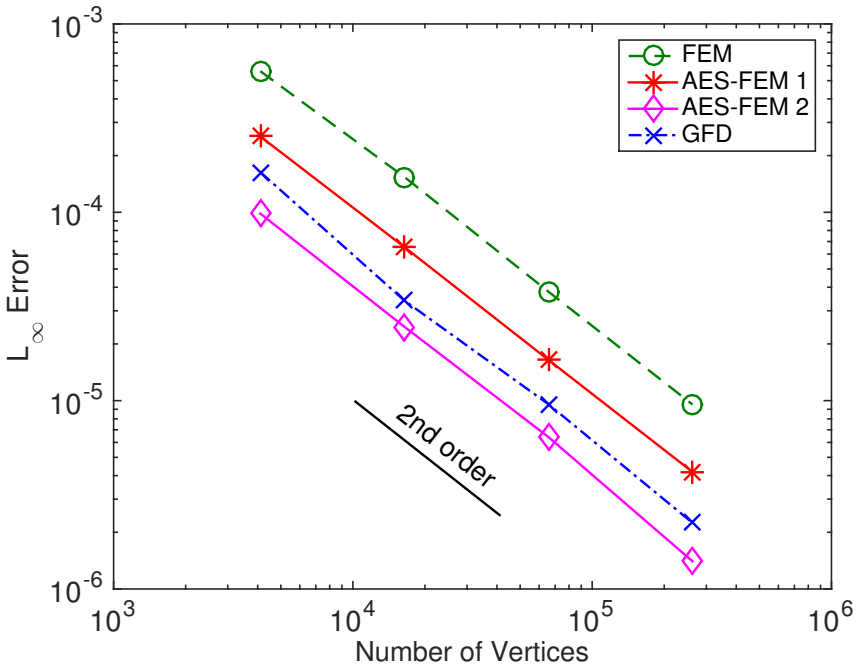

Convection-diffusion equation

$$-\nabla^2 u + c \cdot \nabla u = f \quad \text{in } \Omega$$
$$u = g \quad \text{on } \partial\Omega$$

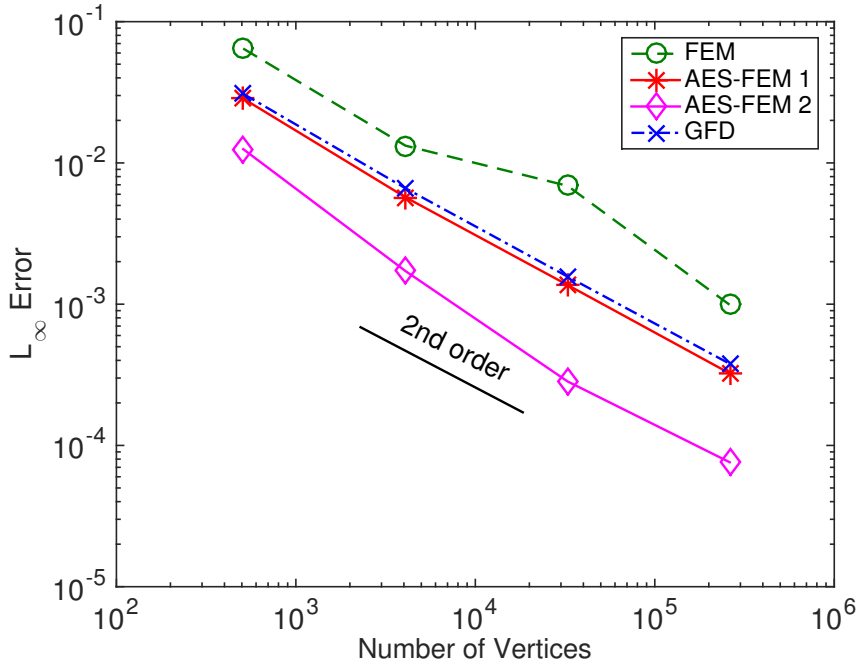

- AES-FEM is about 10 times more accurate than classical FEM

Comparison of Stability of AES-FEM vs. FEM

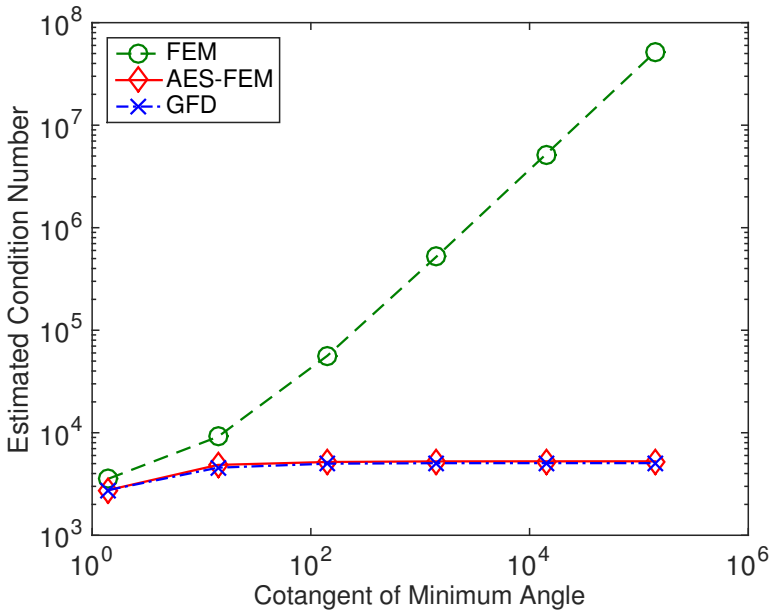

Condition numbers as function of min angles in 3-D

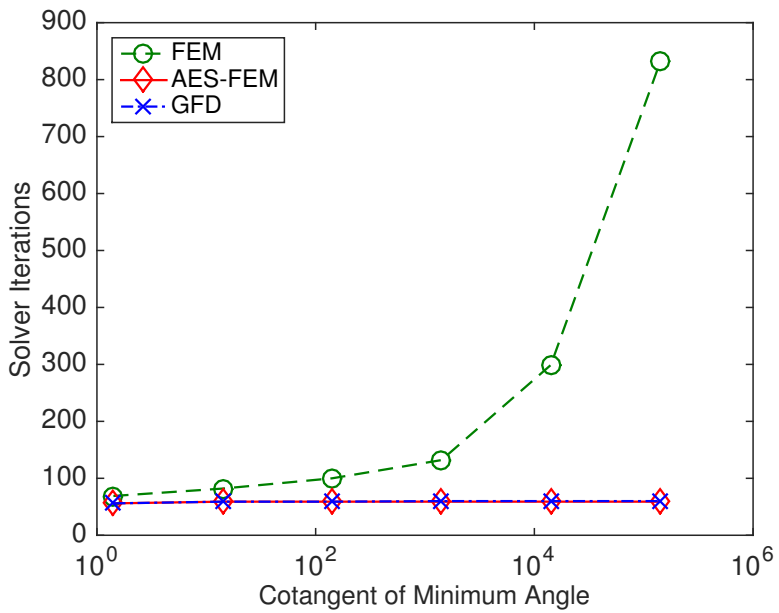

Numbers of solver iterations as function of min angles in 3-D

- Stability (and accuracy) of AES-FEM is independent of element quality

Comparison of Efficiency of AES-FEM vs. FEM

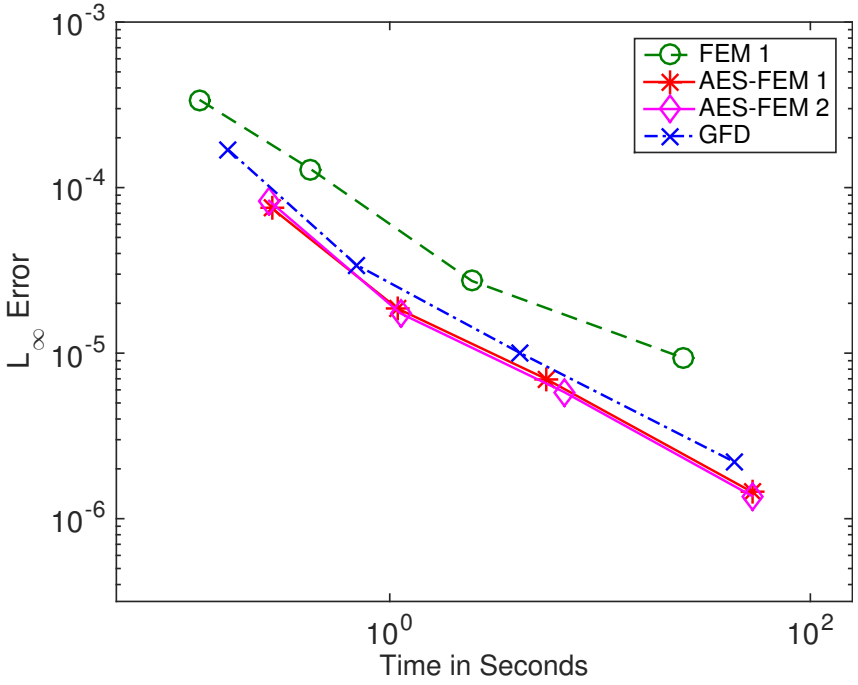

Error vs. runtime for 2D convection-diffusion equation

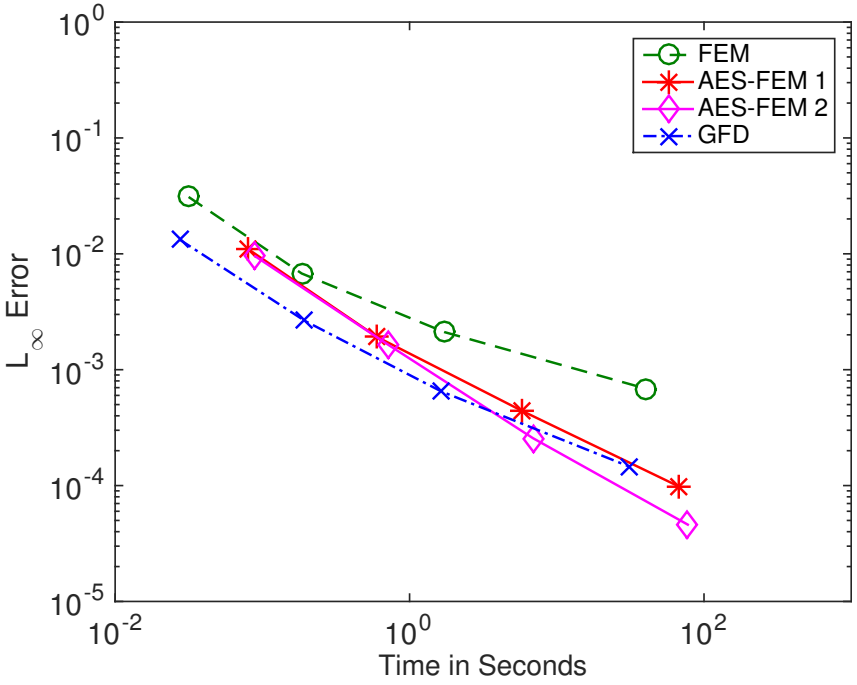

Error vs. runtime for 3D convection-diffusion equation

- AES-FEM is about 2–10 times faster than classical FEM.
- Further optimization of AES-FEM to speed it up by another 2–10 times

High-Order AES-FEM with Linear Elements

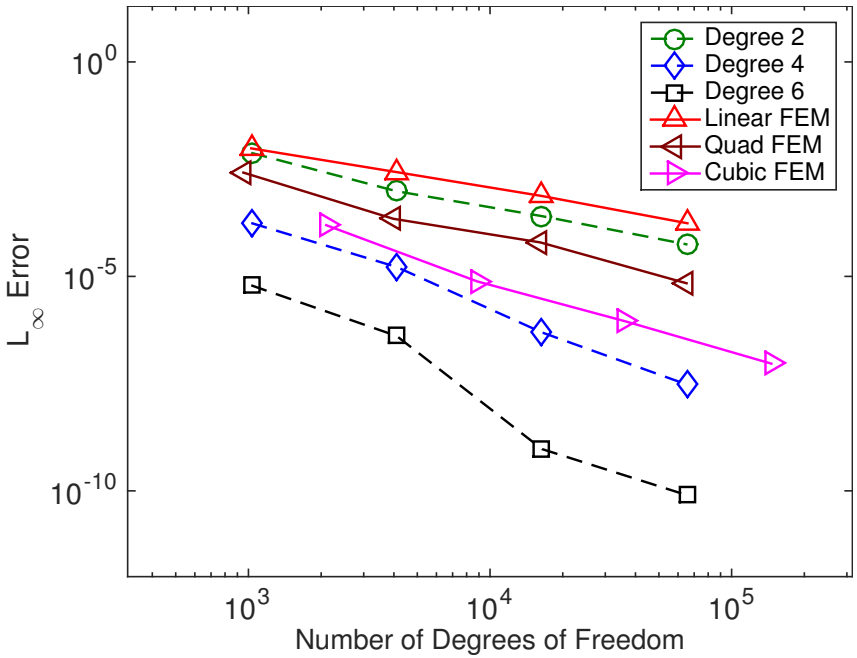

L_∞ errors of AES-FEM and FEM for 2-D Poisson equation

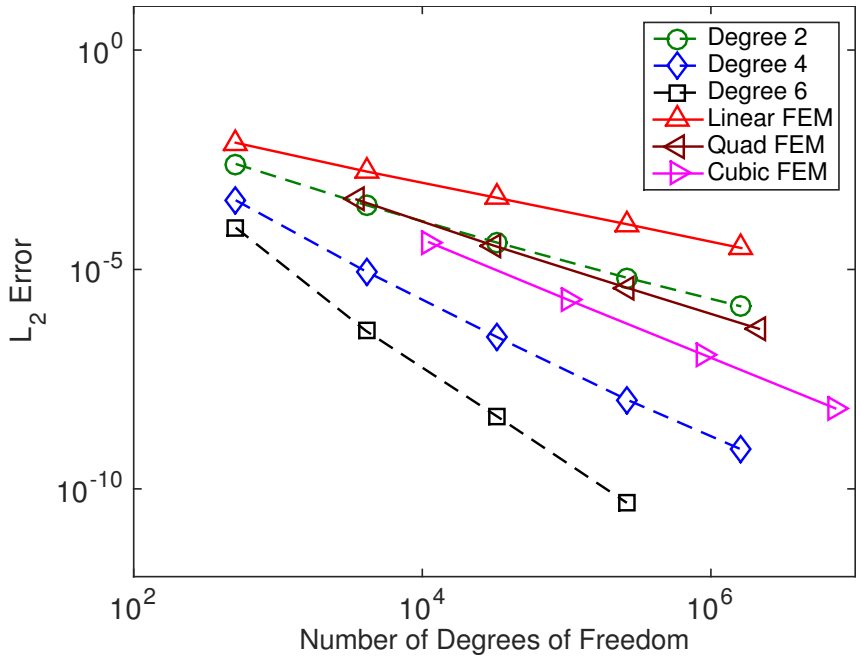

L_2 errors of AES-FEM and FEM for 3-D convection-diffusion equation

- AES-FEM delivers high-order accuracy (up to sixth order in this example) with only linear elements, even poorly shaped elements[3]
- AES-FEM is up to $10,000$ times more accurate than cubic FEM

[3] In preparation for *SIAM J. Sci. Comput.* (*SISC*).

Comparison: Cubic FEM Failed at Meshing for Spheres

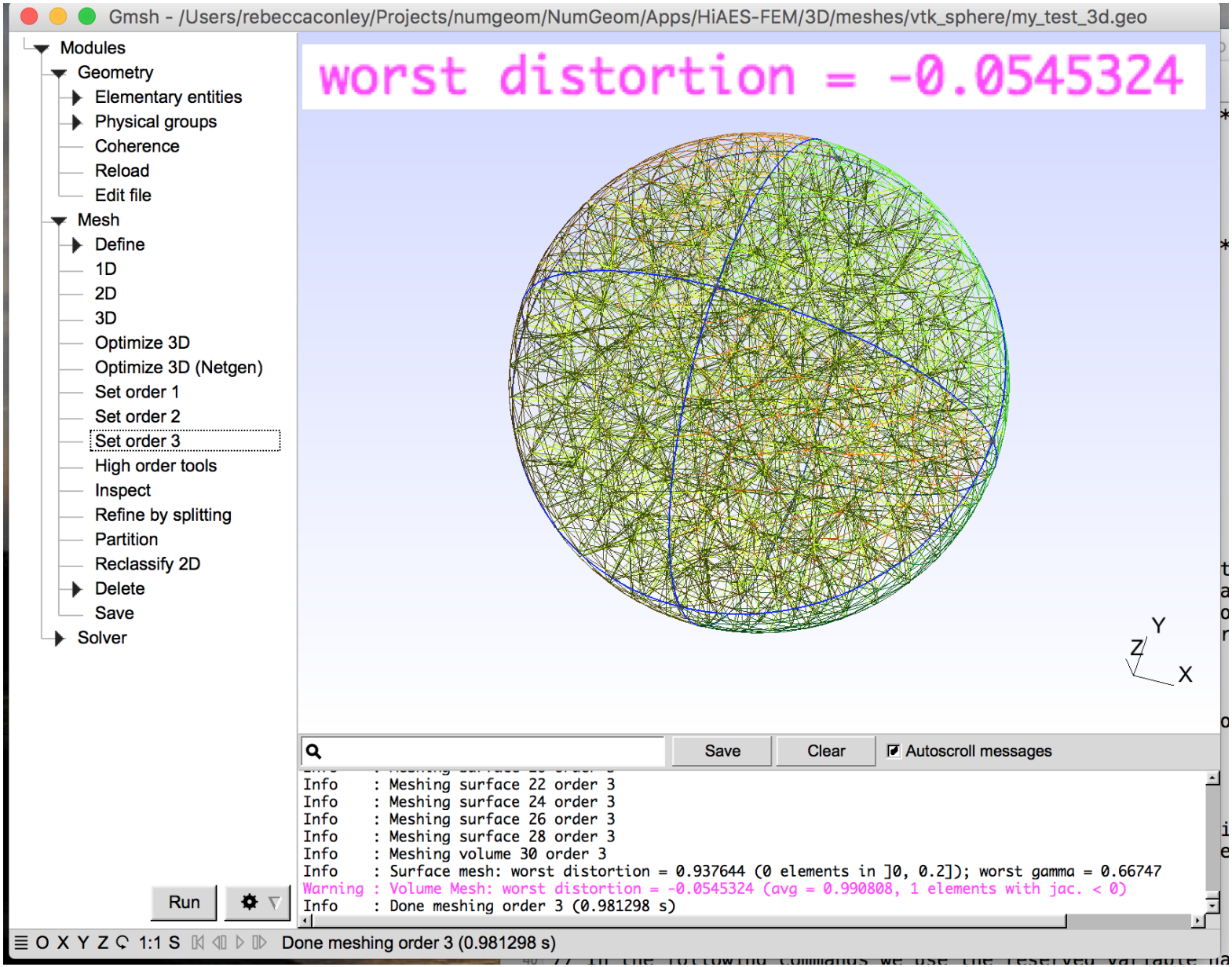

Robust AES-FEM Over Tangled Meshes

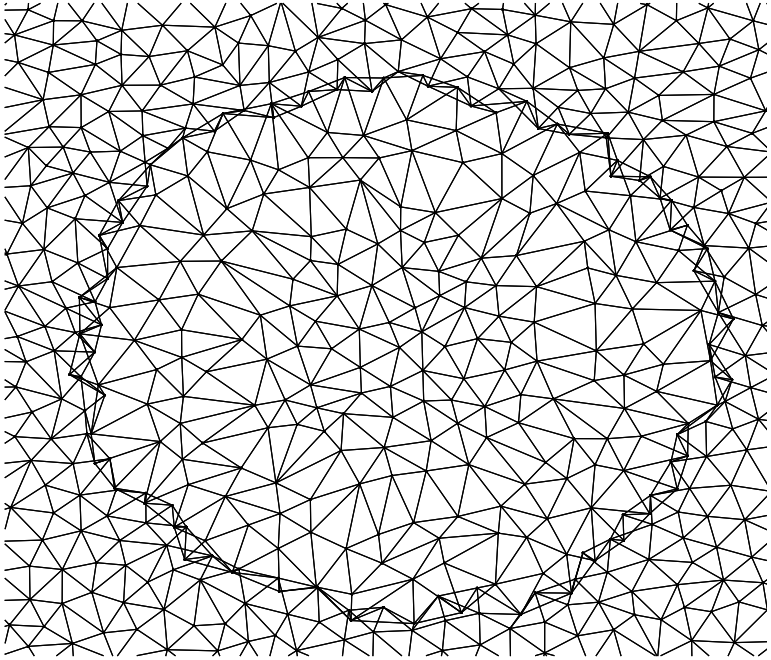

Example mesh with inverted elements

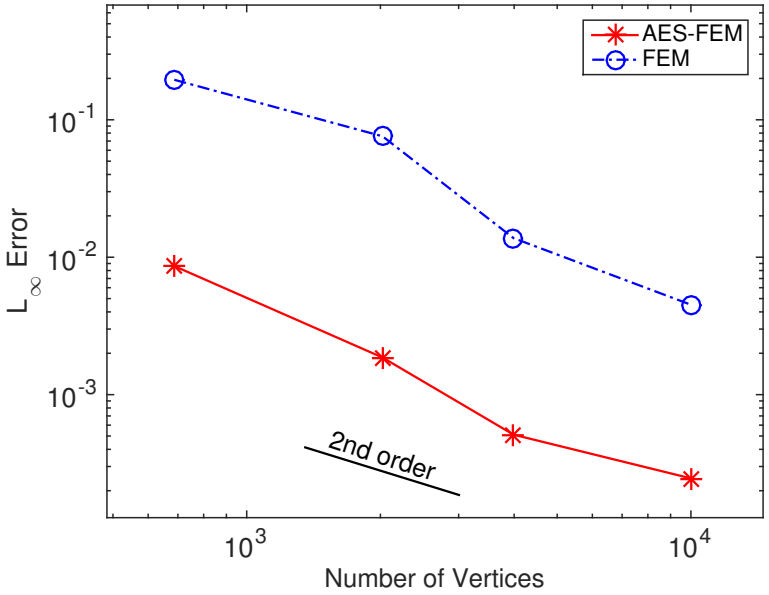

Convergence results of FEM and AES-FEM

- AES-FEM is accurate and stable even over tangled meshes
- This requires adapting stencil and test functions near tangled regions[4]

[4] Work in progress.

WLS-ENO for Hyperbolic Conservation Laws

- We propose WLS-based ENO schemes over unstructured meshes[5]

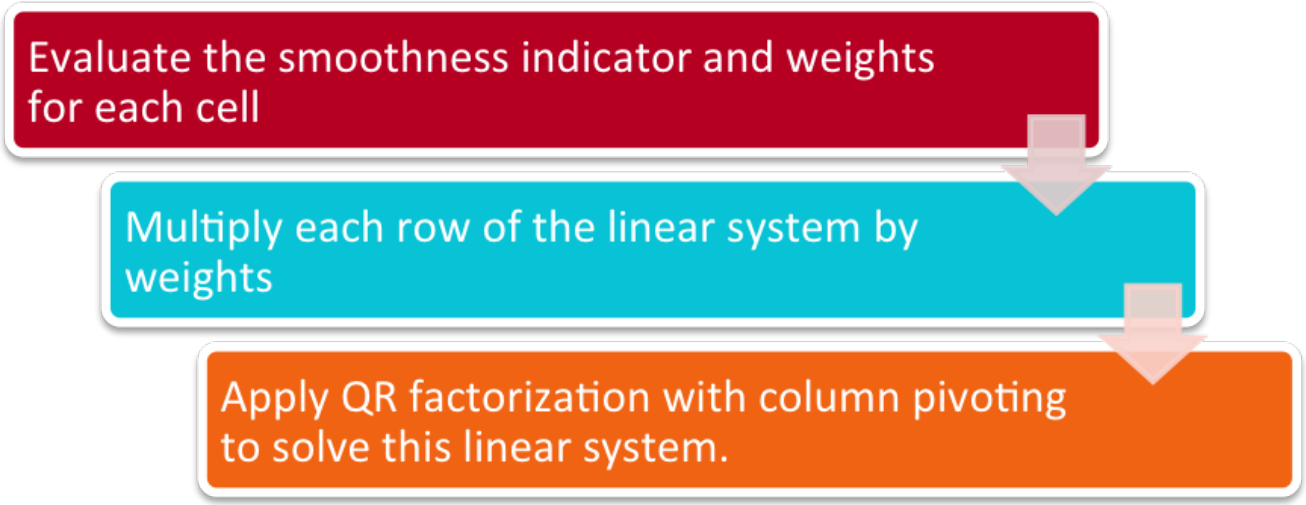

- Works with finite volume and GFD methods
- Advantages over WENO
  - No need to subdivide stencil into sub-stencils
  - No risk of negative weights
  - Better accuracy and stability

[5] H. Liu and X. Jiao, WLS-ENO: Weighted-Least-Squares Based Essentially Non-Oscillatory Schemes for Finite Volume Methods on Unstructured Meshes. *J. Comput. Phys.*, in press, 2016. DOI: 10.1016/j.jcp.2016.03.039.

Example: 1-D Interacting Blast Waves

Consider 1D Euler equation

$$\begin{pmatrix} \rho \\ \rho v \\ E \end{pmatrix}_t + \begin{pmatrix} \rho v \\ \rho v^2 + p \\ v\left(E + p\right) \end{pmatrix}_x = 0,$$

with the following initial condition

$$\boldsymbol{u}\left(x, 0\right) = \begin{cases} \boldsymbol{u}_L, & 0 < x < 0.1 \\ \boldsymbol{u}_M, & 0.1 < x < 0.9 \\ \boldsymbol{u}_R, & 0.9 < x < 1 \end{cases}$$

where

$$\rho_L = \rho_M = \rho_R = 1, v_L = v_M = v_R = 0, p_L = 1000, p_M = 0.01, p_R = 100.$$

Reflective boundary condition is applied at $x = 0$ and $x = 1$.

Results of 1-D Interacting Blast Waves with WLS-ENO

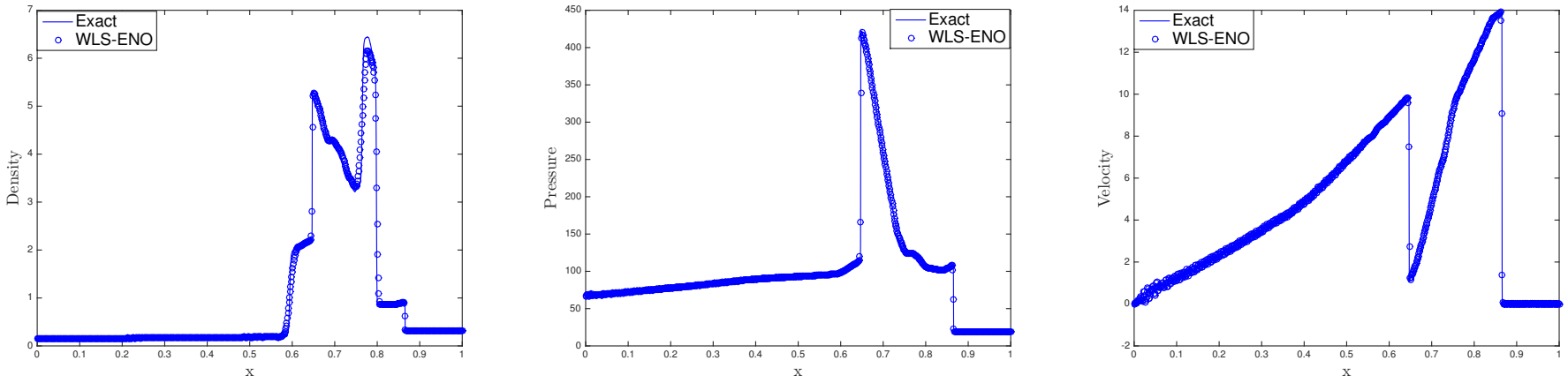

(a) Density. (b) Pressure. (c) Velocity.

Figure: Solutions of at $t = 0.038$ by fifth order WLS-ENO with finite volume method and third-order TVD Runge-Kutta on nonuniform grid.

Example: 3-D Explosion Test

Consider 3-D Euler equations have the form

$$\begin{pmatrix} \rho \\ \rho u \\ \rho v \\ \rho w \\ E \end{pmatrix}_t + \begin{pmatrix} \rho u \\ \rho u^2 + p \\ \rho uv \\ \rho uw \\ u\left(E+p\right) \end{pmatrix}_x + \begin{pmatrix} \rho v \\ \rho uv \\ \rho v^2 + p \\ \rho vw \\ v\left(E+p\right) \end{pmatrix}_y + \begin{pmatrix} \rho w \\ \rho uw \\ \rho vw \\ \rho w^2 + p \\ w\left(E+p\right) \end{pmatrix}_z = 0,$$

with $E = \frac{p}{\gamma-1} + \frac{1}{2}\rho\left(u^2+v^2+w^2\right)$ over unit ball, and initial condition

$$\left(\rho, u, v, w, p\right)^T = \begin{cases} \left(1,0,0,0,1\right)^T & \sqrt{x^2+y^2+z^2} \leq 0.2 \\ \left(0.125,0,0,0,0.1\right)^T & \sqrt{x^2+y^2+z^2} > 0.2 \end{cases}$$

Results of 3-D Explosion Test

Figure: Cross section of ρ in xy plane with 3rd-order WLS-ENO at $t = 0.1$.

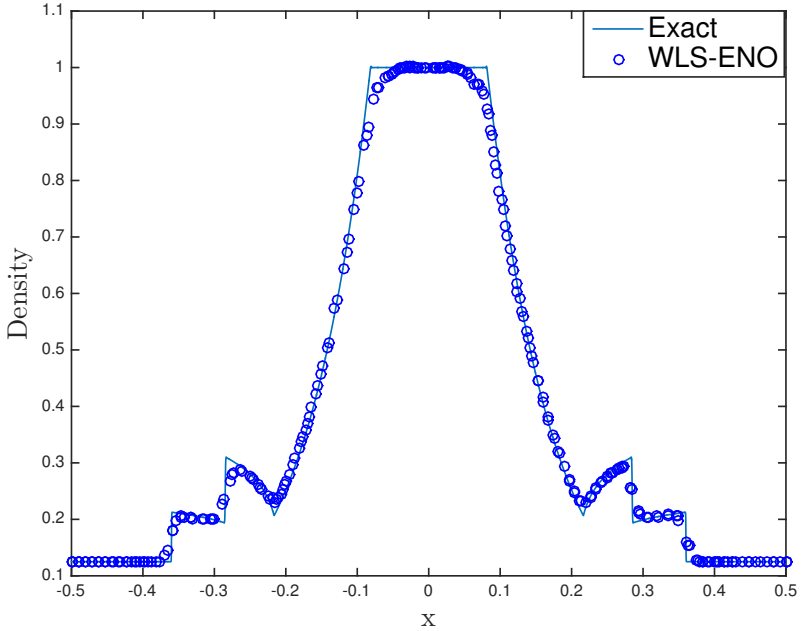

Figure: Solution along x with 3rd-order WLS-ENO at $t = 0.1$.

Outline

Are Geometry and Mesh Generation Important?

- AES-FEM and WLS-ENO change how we look at meshing
  - Element shapes should not be as important for **stability**
  - Isoparametric elements are not necessary for high-order **accuracy**
  - Mesh generation for FEM should not be as hard as it has been!
- Geometry and mesh generation remain important!
  - **Geometric accuracy** is critical for overall accuracy of PDE solutions
  - **Adaptive mesh density** is important for bounding errors
  - **Semi-structured meshes** can lead to nearly optimal discretizations
  - **Hierarchical meshes** can lead to nearly optimal linear solvers
- In contrast, meshless methods throw away geometry and mesh, leading to lower accuracy and lower efficiency

Illustration of Importance of Geometric Accuracy

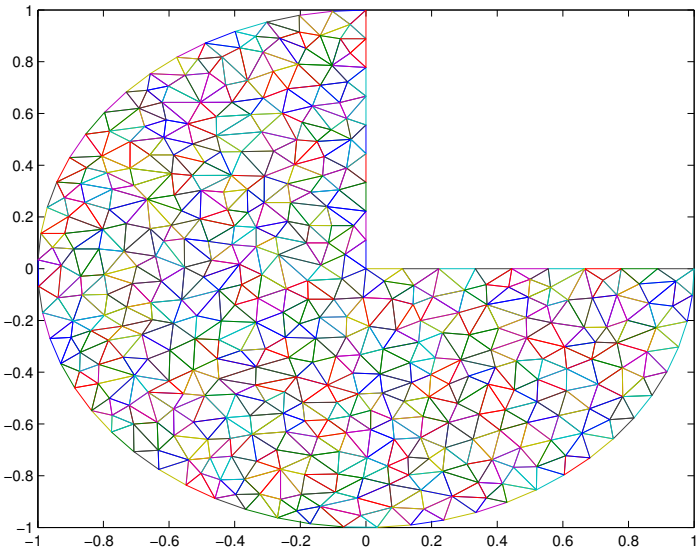

Example curved mesh to undergo grid refinement

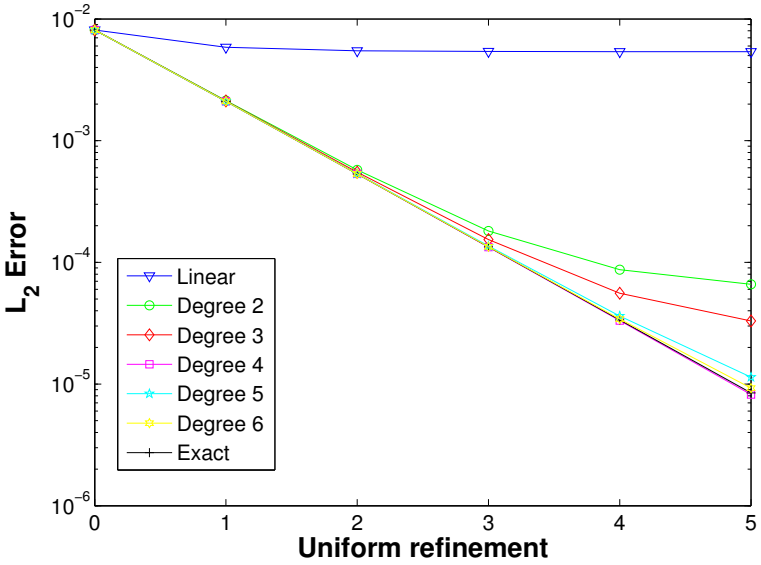

Error of Poisson equation with different geometric accuracy

- Overall solution error may be dominated by geometric error, independently of order of PDE solvers
- Geometry should have sufficient accuracy relative to PDE discretization. Exact geometry is typically not necessary

Illustration of Importance of Meshing on Linear Solver

Timing results (in seconds) for FEM, with PCG as reference.

test case		AMG($L+1$)		GMG	HyGA: Hybrid Multigrid			PCG
verts	L	setup	solve	solve	(2,L-2)	(3,L-3)	(3,L-2)	(ichol)
36K	5	0.15	0.74	0.16	0.36	0.20	**0.14**	1.27
147K	6	0.63	3.68	0.65	1.52	0.90	**0.58**	11.1
32K	3	0.37	1.79	**0.38**	0.42	**0.38**	**0.39**	0.44
292K	4	3.98	24.5	**5.66**	7.32	**5.71**	**5.77**	9.32
2.5M	5	28.5	509	**58.3**	89.5	**59.2**	**59.8**	186

- With 2–3 levels of mesh hierarchy, multigrid solver can be sped up more than 10 times[6]

[6] C. Lu, X. Jiao, and N. Missirlis, A hybrid geometric+algebraic multigrid method with semi-iterative smoothers, *Num. Lin. Alg. Appl.*, Vol. 21(2), pp. 221–238, 2014.

WLS-Based High-Order Geometry

- WLS polynomial fittings under local parameterization
- Let $\varphi(\boldsymbol{u})$ denote smooth bivariate function with local coordinates center at a vertex
- Approximation to $(d+1)$st order of accuracy about vertex by Taylor series expansion

$$\varphi(\boldsymbol{u}) = \underbrace{\sum_{p=0}^{d} \sum_{j,k\geq 0}^{j+k=p} c_{jk} \frac{u^j v^k}{j!k!}}_{\text{Taylor polynomial}} + \underbrace{\sum_{j,k\geq 0}^{j+k=d+1} \tilde{c}_{jk} \frac{\tilde{u}^j \tilde{v}^k}{j!k!}}_{\text{remainder}},$$

where $c_{jk} = \frac{\partial^{j+k}}{\partial u^j \partial v^k} \varphi(\mathbf{0})$

- Fitting to set of data points (u_i, v_i, φ_i) for $i = 1, \ldots, m-1$

$$\sum_{p=0}^{d} \sum_{j,k\geq 0}^{j+k=p} \left(\frac{u_i^j v_i^k}{j!k!} \right) c_{jk} \approx \varphi_i$$

- Solve using weighted least squares

Normal and Curvature over Discrete Surfaces[7]

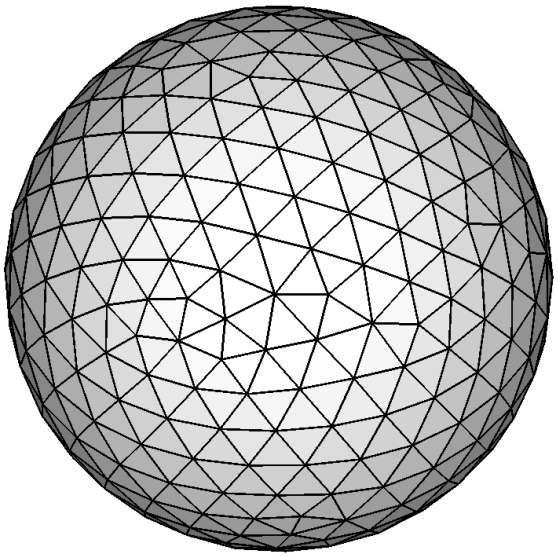

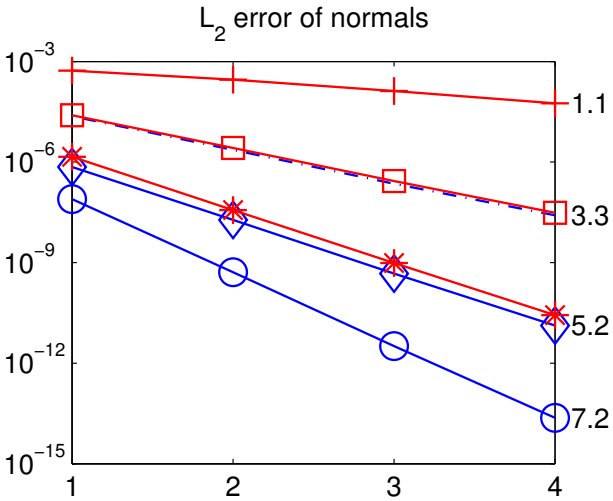

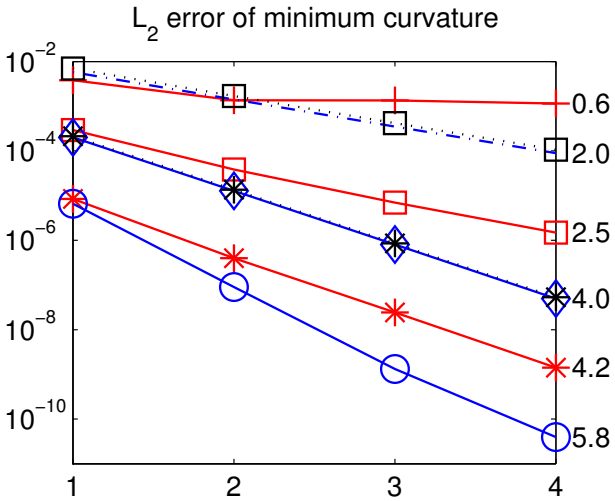

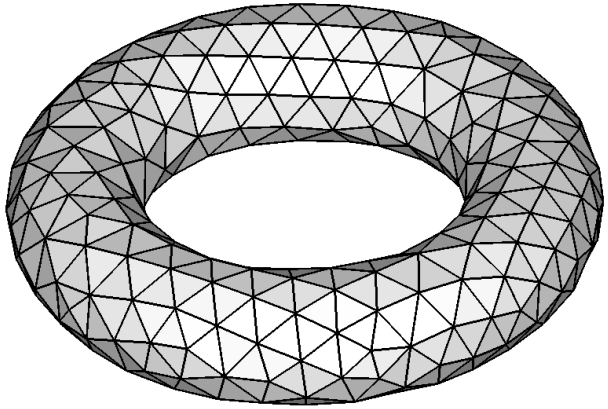

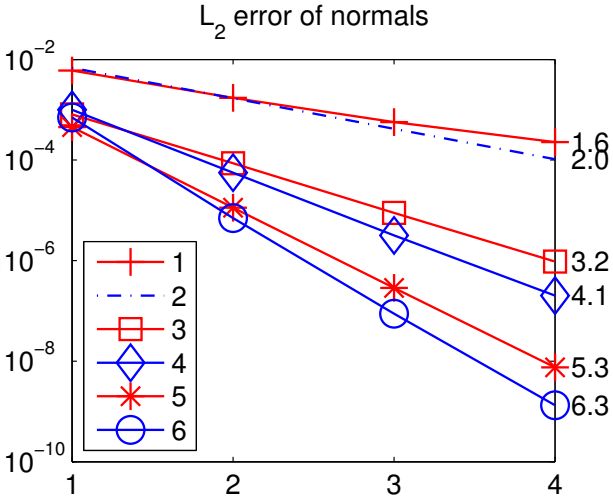

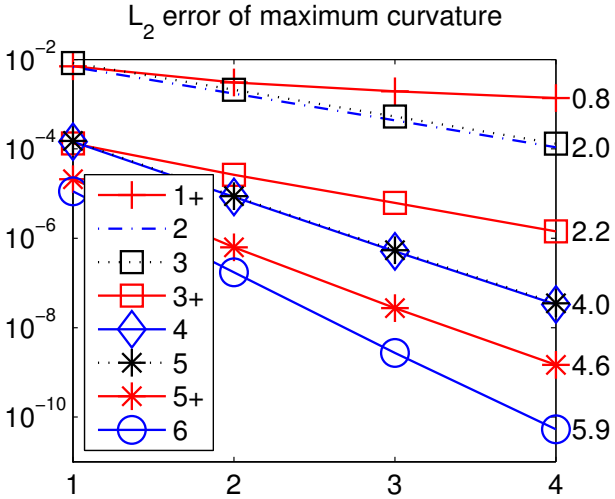

[7] X. Jiao and H. Zha, Consistent Computation of First- and Second-Order Differential Quantities for Surface Meshes, In *ACM Solid and Physical Modeling Symposium*, 2008.

Weighted Averaging of Local Fittings (WALF)[8]

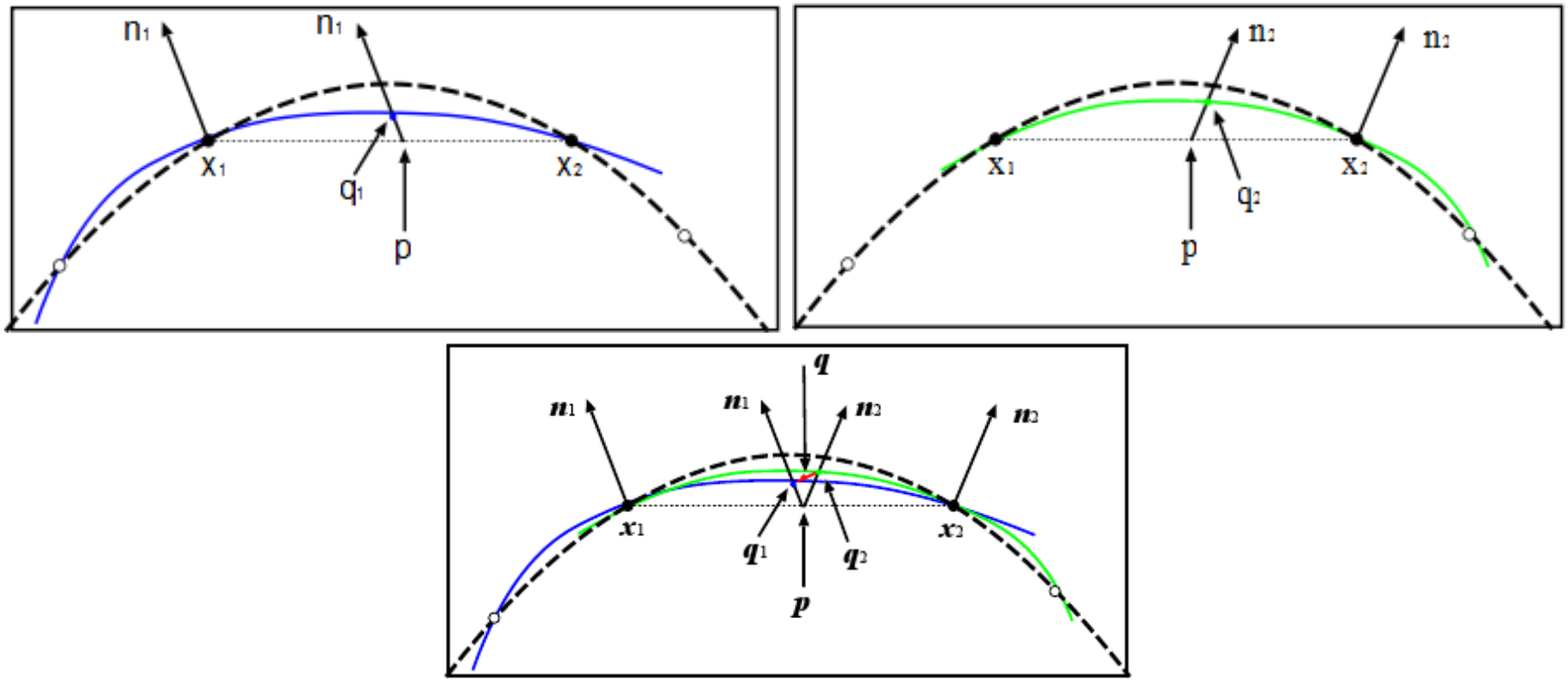

Weighted average enforces C^0 while preserving up to sixth-order accuracy

[8] X. Jiao and D. Wang, Reconstructing High-Order Surfaces for Meshing, *Engineering with Computers*, Vol. 28, pp. 361-373, 2012.

Numerical Accuracy with Mesh Optimization

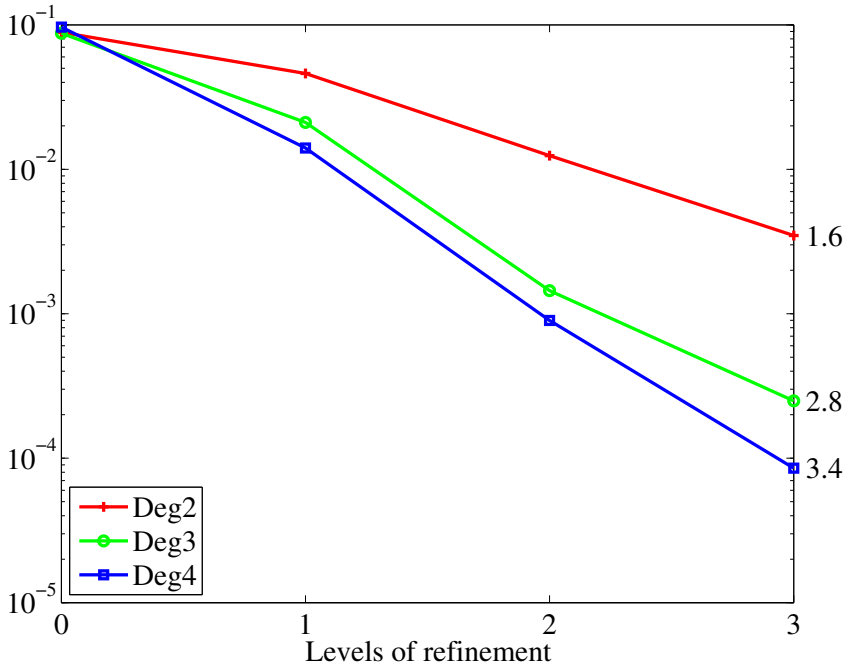

(a) Normals.

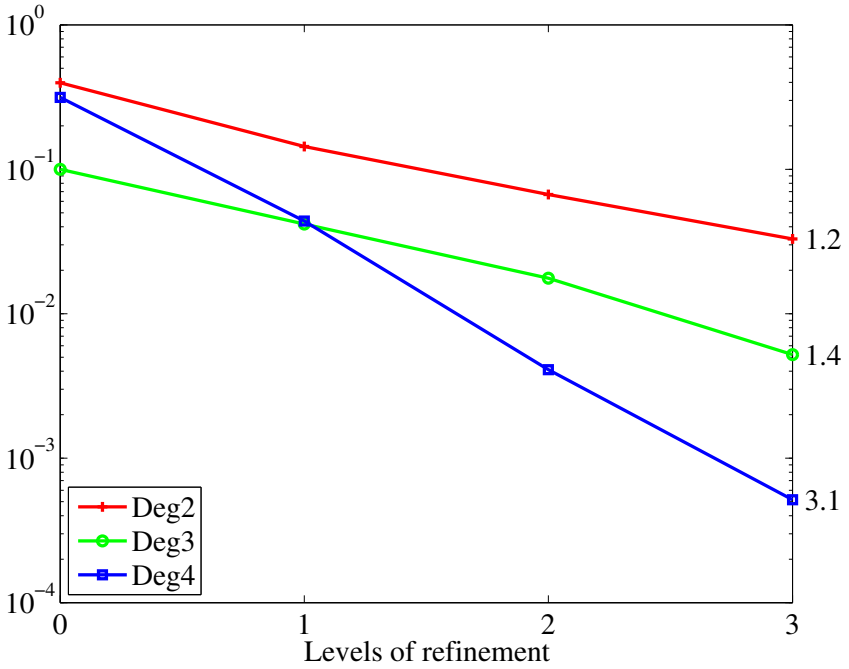

(b) Mean curvatures.

L_∞ errors and orders of convergence of normals and curvatures after mesh optimization for an ellipsoid.

Hermite-Style Least Squares Approximations

- Take into account both position and normal as input
  - Convert normal into derivative of local height function in local coordinate system
  - Construct WLS to minimize Sobolev norm
  - Special treatment needed for reconstructing feature curves and enforcing C^0 continuity across feature curves
- Advantages
  - More compact neighborhood and hence better accuracy
  - Better robustness for coarse meshes

Example Hermite-Style Curve Reconstruction

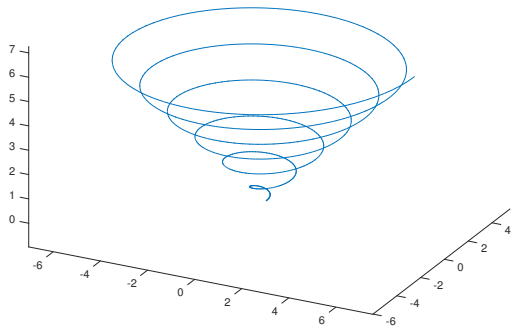

Example conical helix

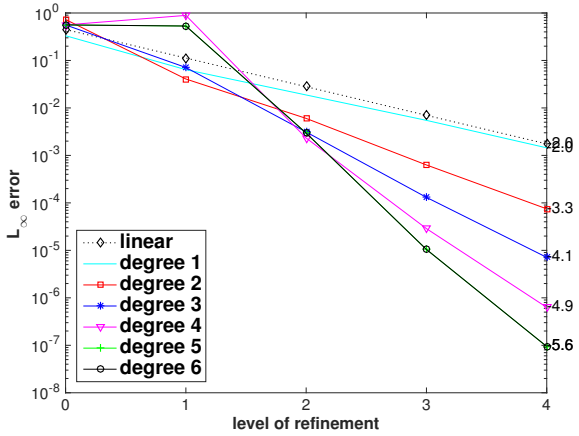

WALF reconstruction

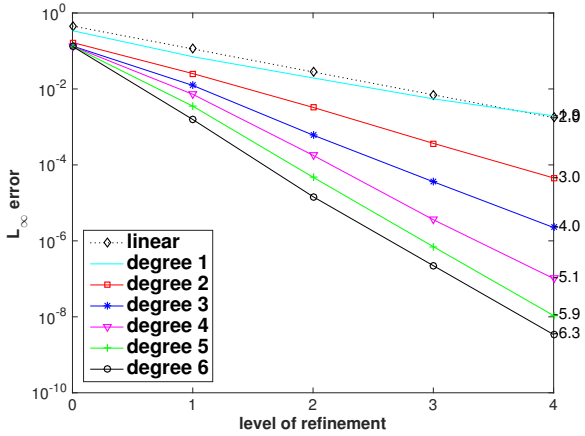

Hermite-style reconstruction

- Hermite-style reconstruction is more accurate
- Hermite-style reconstruction is more robust for coarse meshes

Example Hermite-Style Surface Reconstruction

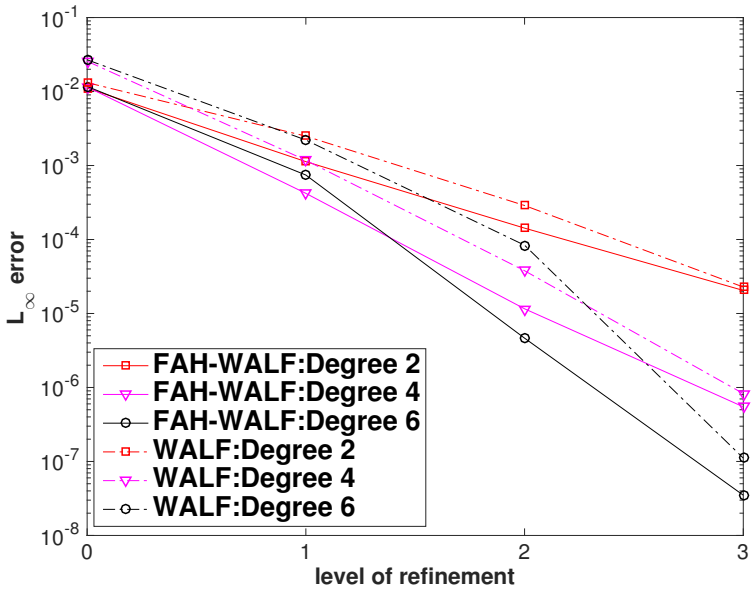

(a) L_2 error of two methods for initial torus mesh with 336 triangles

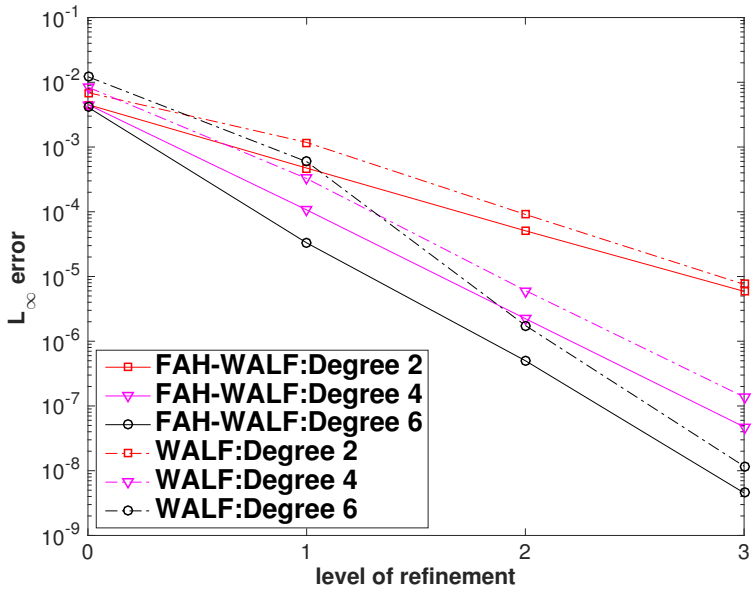

(b) L_2 error of two methods for initial torus mesh with 608 triangles

- Hermite-style reconstruction is more accurate
- Hermite-style reconstruction is more robust for coarse meshes

Outline

Conclusions of WLS Framework

- WLS offers a unified mathematical framework
  - Numerical discretizations of PDEs
  - High-order geometry for meshing
- WLS changes how we consider geometry and meshing
  - Geometric accuracy is important for solution accuracy, but exact geometry is typically not needed
  - Hermite-style reconstruction delivers high accuracy and reliability
  - Meshing should not be responsible for stability of PDE discretizations
  - Meshing still has significant impact of accuracy (point density) and efficiency (point distribution and mesh hierarchy)

CFD Technology Roadmap Revisited (I)

- Mesh generation "remains one of the most important **bottlenecks**"
  - Largely numerical artifacts due to traditional FEM & FVM formulations, which are overly restrictive
  - Can be dramatically simplified by rectifying formulations of FEM & FVM and relaxing mesh-quality dependence
- "**Curved mesh elements** for higher order methods"
  - Curved elements are unnecessary for high-order accuracy
  - Curved isoparametric elements are not optimal in accuracy
- For high-order methods "**robustness** and **cost** considerations remain"
  - AES-FEM offers accuracy, robustness, and efficiency, even with poor-shaped and tangled elements
  - WLS-ENO offers promising solution for hyperbolic conservation laws

CFD Technology Roadmap Revisited (II)

- "**Near optimal**" solvers, including extension of "Krylov methods, highly parallel multigrid methods"
  - Krylov methods and algebraic multigrid are far from optimality
  - Geometric multigrid on few levels of mesh hierarchy enables near optimal complexity and scalability
- "**Disruptive ideas** such as anisotropic cut-cell meshes"
  - Hybrid mesh is key to optimal efficiency in meshing and discretization
  - Disruptive ideas are needed not only to transform mesh generation, but more fundamentally, numerical methods
- "**Tight CAD coupling** and production AMR"
  - Not only tighter integration of geometry and meshing, but also with research in discretization methods, and linear/nonlinear solvers
  - Tight integration in terms of not only software, but also research and theoretical foundation

Future Research Directions

- Parallel implementation of AES-FEM
- Performance optimization of AES-FEM with hybrid meshes
- Implementation of ALE for AES-FEM
- WLS-ENO for generalized finite difference (GFD)
- Multi-physics applications

NumGeom Group Members

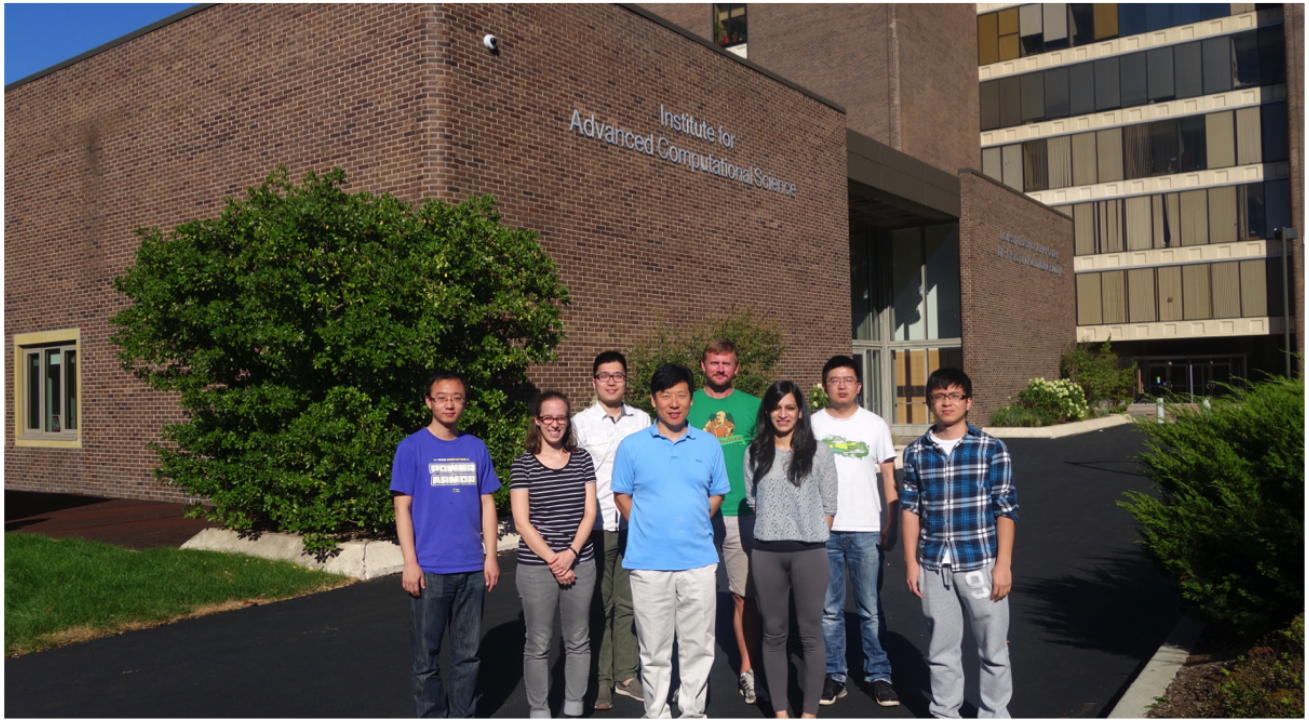

- Past members: Drs. Ying Chen, Bryan Clark, Vladimir Dyedov, Navamita Ray, Duo Wang
- Current members: Hongxu Liu, Rebecca Conley, Xuebin Wang, Prof. Xiangmin Jiao, Tristan Delaney, Aditi Ghai, Cao Lu, and Xinglin Zhao
- Supported in part by NSF, DOE, NIH, and ARO